Experimental realization of the Ehrenberg-Siday thought experiment: Supplementary Material

Giulio Pozzi,[1,2] Chris B. Boothroyd,[1] Amir H. Tavabi,[1] Emrah Yücelen,[3] Rafal E. Dunin-Borkowski,[1] Stefano Frabboni,[4,5] and Gian Carlo Gazzadi[5]

[1)] *Ernst Ruska-Centre for Microscopy and Spectroscopy with Electrons and Peter Grünberg Institute, Forschungszentrum Jülich, D-52425 Jülich, Germany*

[2)] *Department of Physics and Astronomy, University of Bologna, viale B. Pichat 6/2, Bologna, 40127, Italy*

[3)] *FEI Company, Achtseweg Noord 5, 5600 KA, Eindhoven, The Netherlands*

[4)] *Department FIM, University of Modena and Reggio Emilia, via G. Campi 213/a, Modena, 41125, Italy*

[5)] *CNR-Institute of Nanoscience-S3, via G. Campi 213/a, Modena, 41125, Italy*

(Dated: 7 February 2016)

Additional experimental data about the specimen and theoretical simulations showing the effect of an enclosed magnetic flux on a Fraunhofer two-slit interference fringe pattern are reported. Further details about the realization of the Ehrenberg-Siday effect, *i.e.*, the displacement of interference fringes with respect to the diffraction envelope, are presented in the form of a direct measurement of interference fringe position relative to the diffraction envelope. The observations are consistent with symmetry arguments based on theoretical simulations presented in the paper.

I. SPECIMEN DATA

Figure S1 reports the dimensions of the deposited squares and Co bars, measured using scanning electron microscopy (SEM) and atomic force microscopy (AFM).

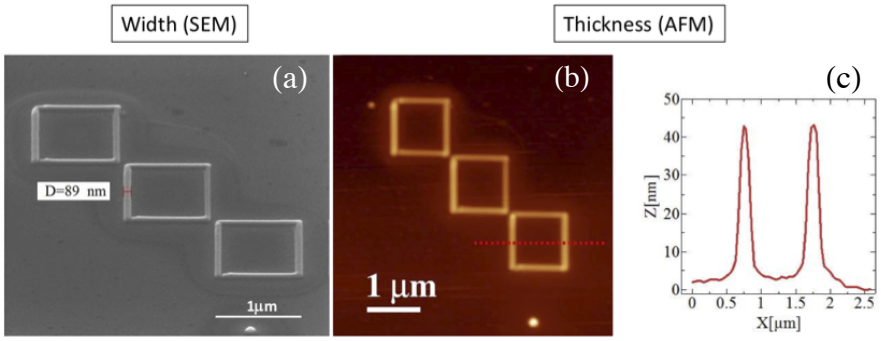

FIG. S1. (a) SEM and (b) AFM images showing the dimensions of the squares and Co bars. (c) is a line scan obtained along the dashed line in (b).

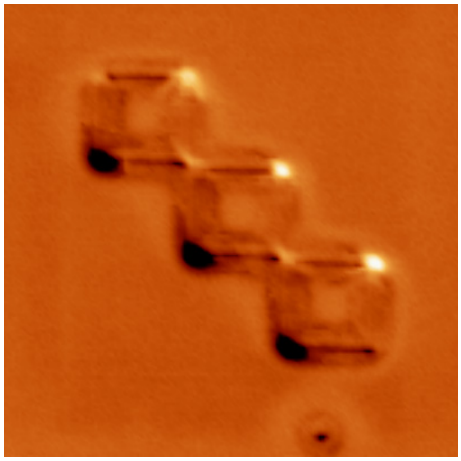

FIG. S2. MFM images of the magnetized square.

Figure S2 shows a magnetic force microscopy (MFM) image of the squares. The image was recorded at remanence after applying a 0.4 T field along the horizontal side of the squares. The resulting magnetization shows a so-called onion-like configuration in each square. The magnetization starts from the top-right corner of each square (bright spot) and closes on the bottom-left corner (dark spot), running along the two branches of the square on either side of the diagonal.

II. SIMULATIONS

Figure S3 (a) shows the central part of a simulated Fraunhofer diffraction pattern of two bare slits, *i.e.*, a diffraction envelope modulated by two-beam interference fringes. The corresponding line profile in Fig. S3 (b) shows that the intensity modulation is rather broad. The images were calculated for slits of width 45 nm, length 480 nm and separation 500 nm. The accelerating voltage was taken to be 300 kV and the focus of the point illumination 50 mm before the specimen. The observation plane was 40 mm from the specimen and the image dimensions are 3 μm $\times$ 1μm. Partial coherence effects due to finite source dimensions were not included.

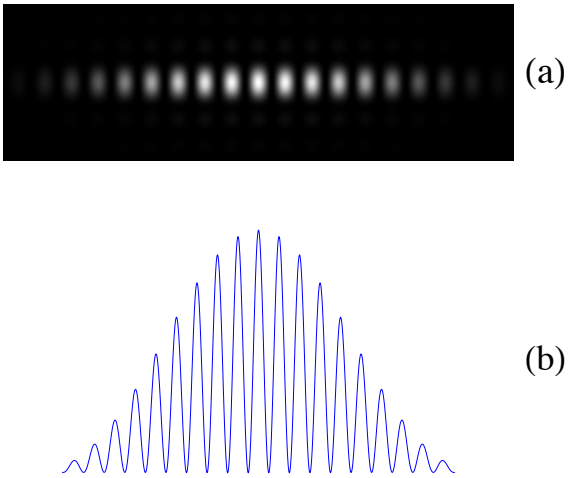

FIG. S3. Simulation of two-beam interference fringes within the central diffraction envelope for two bare slits: (a) intensity distribution; (b) line scan.

The effect on the interference fringe system of a constant magnetic phase shift due to an enclosed magnetic flux is shown in Fig. S4, in which line profiles are reported for phase shifts of (a) 0, (b) $\pi/4$, (c) $\pi/2$, (d) $\pi 3/4$ and (e) π. The effect of the phase shift is a lateral displacement of the interference fringes with respect to the diffraction envelope, such that the pattern is no longer symmetric, until the phase reaches π, when the pattern is again symmetric but with the central maximum replaced by a minimum.

As stated in the paper, in order to better detect the shift of the interference fringes, we

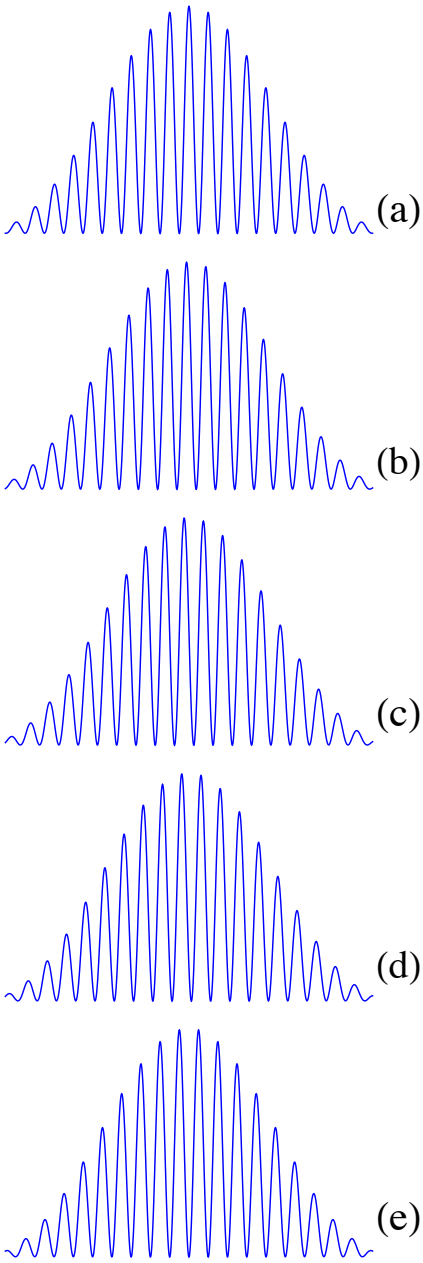

FIG. S4. Simulations of interference images for different values of phase shift between the electron beams: (a) 0, (b) $\pi/4$, (c) $\pi/2$, (d) $\pi 3/4$ and (e) π.

adopted the following procedure. We compared images recorded with opposite magnetization directions by tilting the specimen in the vertical magnetic field of the (weakly excited) objective lens. In this way, the magnetization direction in the rod was oriented by the component of the magnetic field that was in the plane of the specimen and parallel to the direction of the slits and the rod, reversing when the specimen tilt direction was reversed.

Interference fringe images were calculated for opposite phase shifts (corresponding to opposite magnetization directions). The left part of Fig. S5 shows the resulting overlapped line profiles for phase shifts of (a) $\pm\pi/4$, (b) $\pm\pi/2$, (c) $\pm\pi 3/4$ and (d) $\pm\pi$. The right part of Fig. S5 shows the region close to the centre on an amplified vertical scale. The asymmetry in the intensity distributions is better recognized by the fact that the relative maxima of the fringes are of opposite color with respect to the centre. The line scans cannot be overlapped by a simple translation, except for the case of π, when the images are equal but with a minimum at the centre instead of the maximum present in the bare case (Fig. S3).

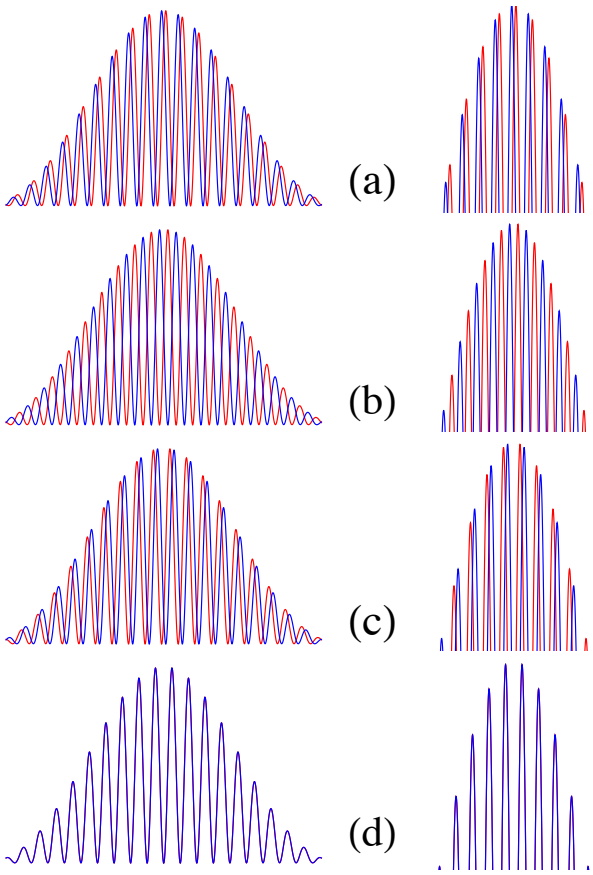

FIG. S5. Simulations of overlapping interference fringes for different opposite values of the phase shift between the electron beams: (a) $\pm\pi/4$, (b) $\pm\pi/2$, (c) $\pm\pi 3/4$ and (d) $\pm\pi$.

This behaviour is illustrated in Fig. S6, which is calculated for the cases $\pi/4$ and $\pi/2$, in which one of the fringe systems has been translated rigidly until the fringes and not the

diffraction envelope overlap. An asymmetrical intensity distribution still remains, confirming that the two images are not related by a rigid translation.

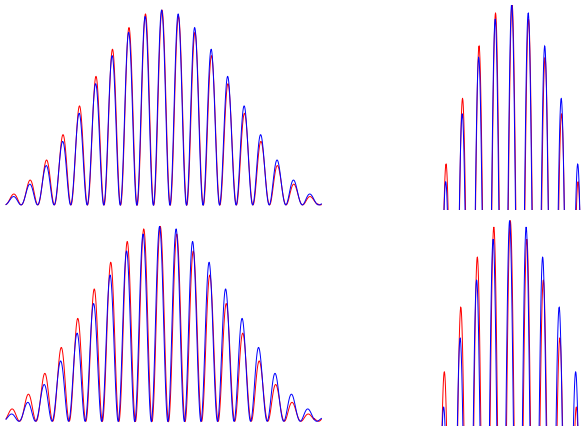

FIG. S6. Simulations of overlapping interference fringes, with the fringes translated rigidly so that they are in registry, for values of the phase shift between the electron beams of $\pm\pi/4$ (top) and $\pm\pi/2$ (bottom). As before, the right part of the figure shows the central region on an amplified vertical scale.

III. MEASUREMENT OF INTERFERENCE FRINGE POSITION RELATIVE TO THE DIFFRACTION ENVELOPE

The effect of a reversal in the magnetisation direction of the Co rod is to shift the interference fringes arising from the two slits, while the diffraction envelope associated with the shape of each slit should remain stationary. However, there are a number of effects that may cause the diffraction envelope to move when the specimen stage is tilted, such as a residual magnetisation of the specimen holder, electrical charging of the support film or a drift of any of the coils or lenses in the microscope. In order to be sure that the interference shift that we observe in Figs 5 and 6 in the paper is due to the Ehrenberg-Siday effect, we need to measure the position of the diffraction envelope and hence the movement of the interference fringes relative to it.

The diffraction pattern of the two slits is a sinc^2 function resulting from the shapes of the individual slits modulated by sinusoidal fringes from interference between them. In order to measure the position of the diffraction envelope alone, the interference fringes were filtered out by using a low pass Fourier filter (see Fig. S7). This procedure works well, as the sideband

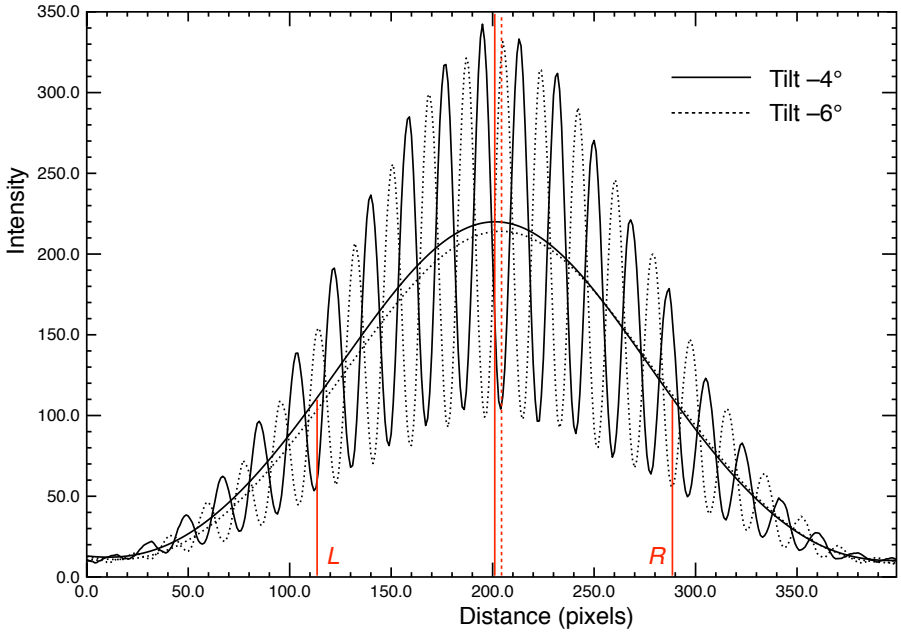

FIG. S7. Projected experimental diffraction patterns for specimen stage tilts of -4° from Fig. 5 (c) (solid lines) and -6° from Fig. 5 (d) (dotted lines). The broad peaks show the same diffraction patterns after Fourier filtering to remove the interference fringes, *i.e.*, the diffraction envelope. The position of the diffraction envelope was determined from the mean of the half maxima positions on the left and right of the broad peak. These positions are labeled L and R for the -4° profile. The position of each diffraction envelope, calculated from the mean of the values L and R, is shown using solid and dotted vertical lines for the two specimen stage tilts.

peaks from the interference fringes in the Fourier transform of the diffraction pattern are well separated from the central peak. Once filtered, the position of the broad diffraction envelope (marked by solid and dotted vertical red lines in Fig. S7) was determined as the mean of the positions of the half-maxima on either side of the peak (L and R on Fig. S7).

It can be seen from Fig. S7 that the movement of the diffraction envelope (red vertical lines on Fig. S7) by 2.8 pixels is much less than the movement of the interference fringes by 10.5 pixels, resulting in a movement of the interference fringes by 7.7 pixels relative to the diffraction envelope.

We repeated the same analysis procedure to determine the position of the diffraction envelope for every frame of the movie shown in Fig. 6 in the paper. The position of the centre of the diffraction envelope is shown by the red line in Fig. S8. Although the

diffraction envelope moves slightly as the specimen stage is tilted, this movement is less than the movement of the interference fringes. In addition, at the four stage tilts at which there is a sudden shift in the interference fringe position, there is little movement of the diffraction envelope.

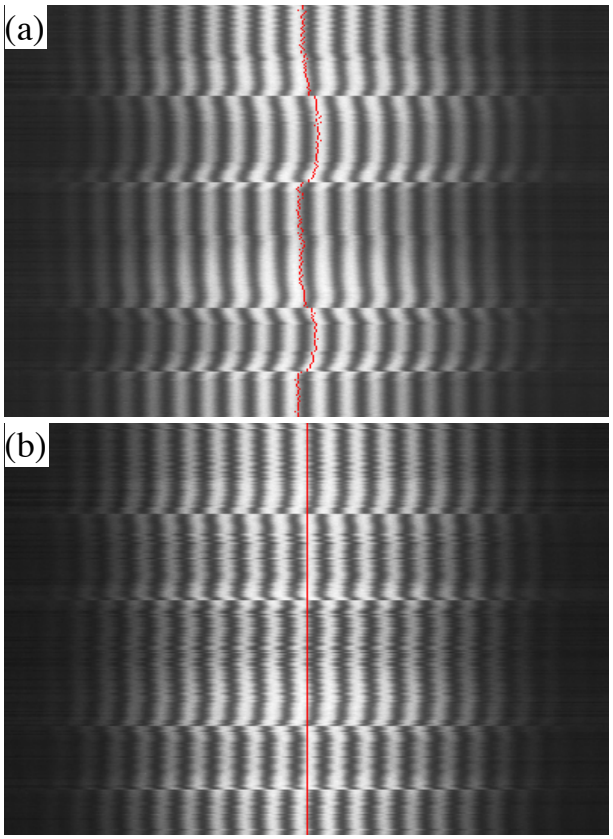

FIG. S8. Projected one-dimensional line profiles extracted from the movie shown in Fig. 6 in the paper, but with the position of the slit diffraction envelope marked by the red line. (a) All line profiles aligned to the same position on the recording CCD camera, as for Fig. 6 in the paper. (b) Line profiles aligned so that the centres of the diffraction envelopes, marked by the red line, are in the centre of the image. The interference fringe shift relative to the diffraction envelope (red line) can be seen clearly.

We have chosen to show the as-measured diffraction patterns in Figs. 5 and 6 in the paper, as this shows the fringe movement due to the Ehrenberg-Siday effect in its simplest form. The detailed analysis given here provides conclusive evidence that the fringe movement shown in Figs. 5 and 6 in the paper is primarily due to the Ehrenberg-Siday effect.

ACKNOWLEDGMENTS

The authors gratefully acknowledge Dr. Alberto Rota (CNR-NANO-S3) for the AFM and MFM images, the European Union Seventh Framework Programme for funding under Grant Agreement 312483-ESTEEM2 (Integrated Infrastructure Initiative-I3) and the European Research Council for an Advanced Grant, number 320832.